

The dynamics of the methanol dissociation at this wavelength are obviously much more complex as compared to photolysis at 193 nm. It seems clear that by simply pumping the molecule to the next electronic state (to the B state as opposed to the A state), the dynamics of the process become significantly more complex. Various processes that appear at 157 nm are in competition with each other, and thus the results here provide a good probe of the electronic surfaces and the processes that occur on them.

In conclusion, photodissociation of a few typical hydrocarbon molecules have been carefully studied using advanced molecular beam techniques. Experimental results show that there are atomic and molecular hydrogen elimination processes from the photodissociation of these typical hydrocarbons at 157 nm. This is especially interesting since almost eight electron volts of energy have been deposited into the molecules through photoexcitation. The selectivity shown in the photodissociation processes of these molecules indicates that photodissociation of medium size molecules may likely a clear dynamics-controlled process rather than a dissociation of statistical nature under high energy photon excitation. It is also believed that electronically excited state could play important roles in the dissociation of these highly electronically excited molecules in which the energy is likely not fully randomized.

### 3. VUV Synchrotron Radiation Based Molecular Beam Apparatus at SRRC

The idea using the tunable VUV ionization from synchrotron radiation to detect reaction products is very appealing. The advantages using this idea to study reaction dynamics have also been discussed in the Introduction. This idea has been realized at the Advanced Light Source in Berkeley, at which a crossed molecular beam apparatus has been setup for chemical dynamics research. Besides the advantages using VUV ionization as a ionization probe, one of the main concerns in this technique is the ionization efficiency using the synchrotron VUV radiation. Let us consider a typical case of VUV ionization using third generation synchrotron radiation. A VUV light beam with a photon flux of  $I_{\text{SRRC}} = 10^{16}$  photons/s is focused in a typical area of about  $1 \text{ mm}^2$  (about 1 mm in ionization length  $l$ ), the light intensity in the ionization region is  $\varphi_{\text{SRRC}} = 10^{18}$  photons/cm<sup>2</sup> s, a typical ionization cross section for a molecule,  $\sigma_{\text{ion}}$ , is about  $10^{-17}$  cm<sup>2</sup>. Ionization probability of a molecule in the ionization region per second is

$$P_1 = \varphi_{\text{SRRC}} \times \sigma_{\text{ion}} = 10 \text{ s}^{-1}.$$

For a reaction product molecule with a typical speed of  $v = 1.0 \times 10^5$  cm/s (resident time  $\Delta t = l/v = 1 \times 10^{-6}$  s), the probability to be ionized in the ionization region,

$$P_i \times \Delta t = 1 \times 10^{-5}.$$

Therefore, the ionization probability in a typical VUV ionizer using synchrotron radiation from a third generation synchrotron radiation light source is comparable to that in a typical electron impact ionizer used in the universal crossed molecular beam apparatus described above. From this analysis, VUV ionization using third generation synchrotron radiation can clearly be applied to chemical dynamics research at least as good as the electron impact ionization method. The first crossed beam apparatus using synchrotron ionization was successfully established in Berkeley. In this chapter, we would like to describe the significantly improved version of a similar apparatus, which is recently established at the Synchrotron Radiation Research Center in Taiwan, and some preliminary results on the photochemistry studies of polyatomic molecules using this apparatus.

### 3.1. Description of the Apparatus

The design principle for the crossed molecular beam machine established at the chemical dynamics beamline in the Synchrotron Radiation Research Center is very much similar to the original version developed at the Advanced Light Source in Berkeley. Many of the features in the apparatus are also quite similar to the universal crossed beam apparatus described above. The use of synchrotron radiation imposes additional design restrictions, associated with the strict vacuum requirements necessary for synchrotron operation and the fact that the ionizing light beam must remain fixed in space. The synchrotron ring at SRRC also requires exceptionally clean vacuum conditions. In addition, since the ionizer must be fixed in space, the beam *sources* must rotate in order to sample different recoil angles. Such a design has been previously developed for a single molecular beam using a fixed diffusion pump.<sup>81</sup>

One of the most important considerations in the design of an instrument such as this one is the differential pumping system which allows for production of intense continuous or pulsed molecular beams in one part (source region) of the machine operating at pressures up to  $10^{-4}$  torr, while maintaining ultra-high vacuum ( $p_{\text{tot}} < 3 \times 10^{-11}$  torr) for a mass-spectrometric detector in another part of the machine. We have chosen magnetically levitated turbo molecular pumps to fulfill the design

requirements. Unlike diffusion pumps these pumps may be mounted in any orientation and move with the rotating sources. Furthermore, since they have no pumping or lubricating fluid, the entire instrument may be made oil-free. Fast-trip gate valves together with differential pumping stages located between the synchrotron ring and the end-station prevent vacuum loss in the molecular beam machine from affecting the synchrotron ring.

An overview schematic of the machine is shown in Fig. 21. Two molecular beam sources, fixed at a  $90^\circ$  crossing angle, rotate together with respect to the detection axis. The molecular beam source assembly can be rotated from  $-20^\circ$  to  $110^\circ$  degrees so that both beams may point into the detector for beam diagnostic purposes. One of the molecular beam sources consists of two separately pumped chambers, a source chamber, pumped by a 2000 L/s magnetic levitated turbo pump, and a differential pumping chamber, pumped by a 300 L/s magnetic levitated turbo pump. Other one only contains a single source chamber, which is pumped by a 1000 L/s magnetic levitated turbo pump, without differential pumping between the source and the main chamber. All these three pumps are attached directly to the rotating source assembly and move when the source is rotated. During operation, the source chamber pressures are typically  $10^{-3}$  torr and the differential pumping chambers are  $10^{-5}$  torr.

The main interaction chamber is a large stainless steel chamber, evacuated by a 2000 L/s turbomolecular pump backed by an oil-free pump station, which holds the rotating source assembly. The main chamber is also cryo-pumped by a He closed cycle refrigerator cryopump for better vacuum. The main chamber pressure is typically  $10^{-8}$  torr during operation. A large square port on the interaction chamber aligns the detector to the rotation axis of the sources and the crossing volume of the molecular beams. The detector has four differentially pumped chambers. The first region (labeled I in Fig. 1) are pumped by two 300 L/s turbomolecular pumps (Seiko Seiki STP300) and reduce the main chamber pressure effusing into the detector to  $\sim 10^{-10}$  torr, respectively. Region II is a dual walled liquid nitrogen dewar, pumped by a 400 L/s turbomolecular pump (Seiko Seiki STP400) and houses the photo-ionization region and ion optics to transport the ions to region III. The ultimate pressure of region II is lower than  $3.0 \times 10^{-11}$  torr, which was the typical operating pressure in region II. Region III holds the quadrupole (Extrel) mass spectrometer and standard Daly ion counter<sup>82</sup> and is pumped by a 300 L/s magnetically levitated turbomolecular pump. All four turbo pumps on the detector are backed up by

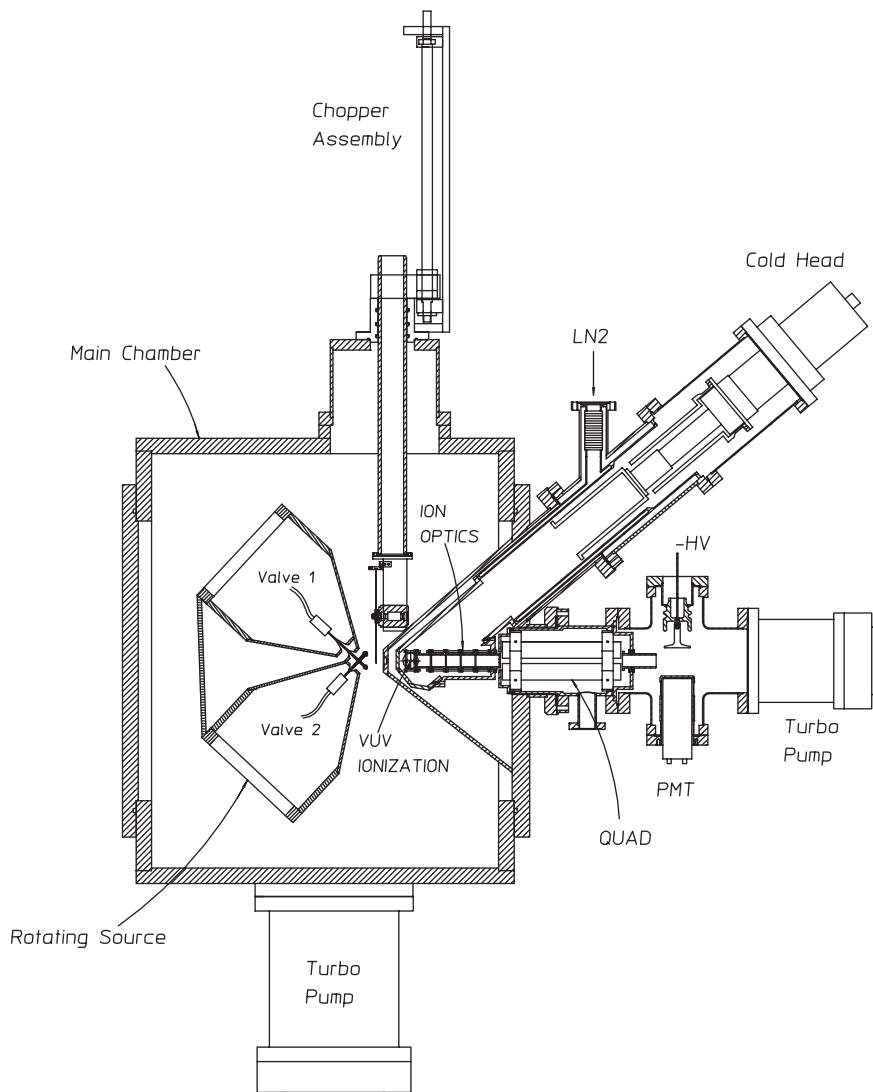


**Fig. 21.** A schematic diagram for the crossed molecular beam apparatus using VUV synchrotron radiation ionization scheme at SRRC.

a 300 L/s magnetically levitated turbo pump, which is then backed up by an oil free pump station.

Despite this extensive pumping scheme, molecules which pass directly through the detector's differential pumping apertures along a line

connecting the beam crossing volume and the ionization volume are immune to differential pumping and then limit the lower level of the background in many experiments. Because the mean free path in the interaction chamber is of kilometer length, these “direct-through” molecules must *desorb* from surfaces which lie in the detector’s viewing window, behind the beam crossing volume. To eliminate these molecules, a cryogenically cooled copper plate is placed behind the molecular beam crossing volume and within the detector viewing window. When cooled to below 30 K, little that adsorbs on this copper plate can desorb into the detector.

Two improvements on the new apparatus over the original version at the ALS are made. In order to increase the detecting sensitivity, the ionization region is moved to 10 cm away from the interaction region, which is much shorter than the 15 cm distance at the ALS apparatus. This will enhance the detection sensitivity by more than 2 times. Certainly, this will scarifice the time-of-flight resolution a little bit, while still acceptable. In a crossed beam apparatus, however, the detection sensitivity is always more important. Another improvement of the new apparatus over the ALS version is the usage of a larger quadrupole rod assembly (1.25 inch diameter), similar to the molecular beam apparatus described above. This could also improve the ion transmission by about 3 times over the similar apparatus at ALS. Overall, this new apparatus should be about 6~7 times more sensitive than the similar apparatus at the ALS in Berkeley.

The Synchrotron Radiation Research Center is one of the third generation synchrotron radiation facilities available in the world, which runs at 1.5 GeV in electron energy. The design of the SRRC is optimized for insertion devices (undulators, wigglers) which produce tunable VUV to soft X-ray radiation with much higher photon flux than bending magnets. These insertion devices, in particular undulators, offer the world’s brightest sources of VUV light with a large duty factor. The raw undulator output is greater than  $10^{16}$  photons/s with a bandwidth  $\Delta\nu/\nu$  of about 2%. The undulator used for the beamline was about 4.5 m in length and had a total of 47 9-cm periods. Since the U9 undulator generates many harmonics with high energy. Special measures must be taken to reduce the intensity of the harmonics. Fortunately, losses on the mirrors needed to guide the undulator output to the crossed molecular beam machine strongly attenuate the contribution from harmonics above 100 eV, and virtually eliminate everything higher than 500 eV, while at the same time directing and focusing the beam as desired. One drawback of thin film filters and mirrors is a transmission gap ranging from the lithium fluoride cut-off at 11 eV to about 35 eV. For

soft photo-ionization, this region is of considerable importance, since the third harmonic dominates the spectrum of the undulator harmonics and 11–12 eV will be frequently used for the fundamental. These considerations prompted us to use a windowless harmonic filter employing rare gas (argon or neon) as the filter medium with differential pumping serving to preserve the beamline vacuum, similar to the original harmonic filter at the chemical dynamics beamline on ALS. For all intents and purposes the higher fundamentals can be removed almost completely with the gas filter.

### 3.2. *Photodissociation Dynamics of Polyatomic Hydrocarbon Molecules*

Since the establishment of the new apparatus last year, it has been used to study photodissociation dynamics of a few polyatomic molecules. In the following sections, we will briefly describe some of the interesting dynamics in the studies of photofragmentation of methyl chloride and cyclopropane at 157 nm. Many of the advantages using tunable VUV ionization are demonstrated in these studies.

#### 3.2.1. *Cyclopropane at 157 nm*

Total four different dissociation channels have been observed.<sup>83</sup> One of the most interesting results is the H atom formation channel. From our measurements, signal at parent mass minus one is not observed at low ionization photon energy. While mass 40 signal and mass signal are clearly now from a same binary dissociation process. Kinetic energy distribution (KED) for the H atom product could be obtained from fitting the TOF spectra (Fig. 22) at mass 1 assuming that the H atom is from a binary dissociation. Signals at mass 40 can also be simulated assuming that the signals are from a binary H atom loss channel. In this way, we assume that parent mass 41 products from the binary H atom elimination are not stable using the VUV ionization and it subsequently cracks to lower mass products. The kinetic energy distributions determined from fitting the TOF spectra at mass 40 and 39 is also shown in Fig. 23, assuming all these signals are from a binary H atom elimination channel. Looking at Fig. 23, the two kinetic energy distributions obtained from mass 1 and mass 40 apparently show very significant differences. This difference seems to come rather from the peculiar dissociation dynamics of the two photofragments.

From Fig. 23, the kinetic energy distribution obtained from the H atom product is clearly too low for a binary H atom dissociation since the lowest

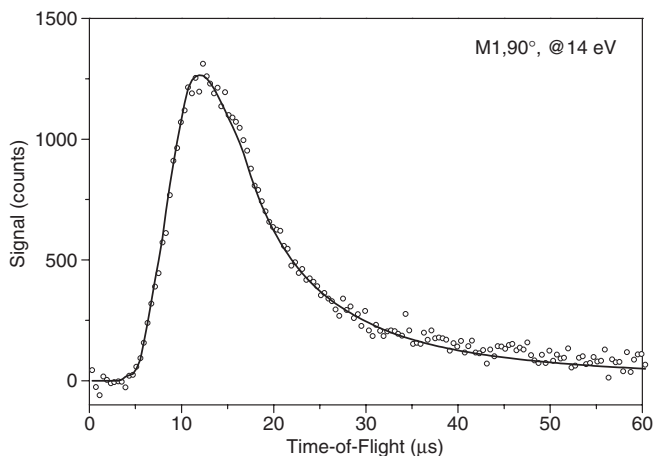


**Fig. 22.** Time-of-flight spectra for the H atom product from photodissociation of cyclopropane at 157 nm.

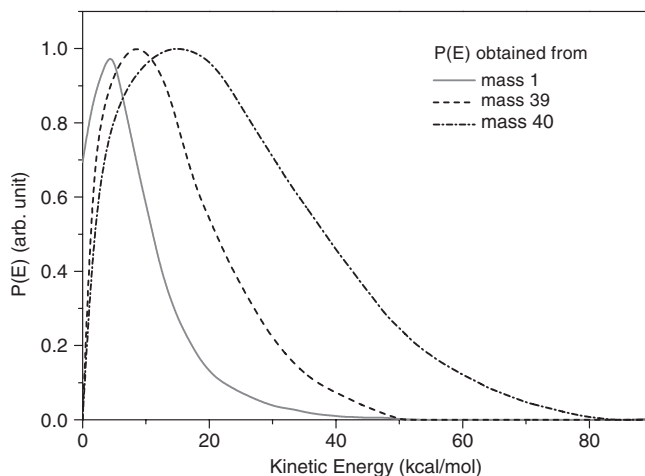


**Fig. 23.** Translational energy distributions obtained from simulating the TOF spectra of the mass 1, mass 39 and mass 40 products from propane photodissociation at 157 nm.

energetic limit for such a process is about 75 kcal/mol, while the observed energetic limit in the KED for H atom product is only about 40 kcal/mol. The energy cut-off limit of the KED obtained from the heavy product at mass 40 is about 80 kcal/mol, about twice of that obtained from the H atom, assuming both products are from a binary H atom elimination channel.

From these analyses, it is not too difficult to conclude that these products could not come from a simple binary H atom dissociation channel simply because kinetic energy distributions for the two products could not match each other. From the energetic limit of the H atom product, the H atom products are more likely coming from a triple product channel in which two hydrogen atoms are eliminated. There are a few possible pathways shown in the energetic diagram: allene ( $=C=C=C$ ) + 2H, propyne ( $CH_3C\equiv CH$ ) + 2H and  $c\text{-}C_3H_4$  + 2H. Energetically, since the cut-off of the KED for the H atom products is about 40 kcal/mol, the H product is likely produced by the first two processes, which have available energies of about 45 kcal/mol, not by the  $c\text{-}C_3H_4$  + 2H process which has an available energy of only 23 kcal/mol. Both reaction pathways involve the ring-opening and new-bond formation processes. For the formation of propyne, additional H-migration process is also needed. Therefore, the allene + 2H dissociation channel might be more favorable than the channel that involves propyne. Energetically, the allene + 2H channel is also slightly more closer to the experimental limit. Such a process could also account for the observation that the mass 40 signals appear to be noticeably faster than a simple binary H atom dissociation because the  $C_3H_4$  radical receives kicks from two H atoms rather than a single H atom. Through the above analysis, a possible mechanism is proposed in which cyclopropane goes through a ring-opening process, then the two H atoms in the middle are eliminated simultaneously. Further and more detailed theoretical and experimental studies are desirable in order to verify this interesting dissociation mechanism.

In addition to the H formation channel, an extra fast feature has been clearly observed in the TOF spectra detected at mass 39. Since  $H_2$  products have been detected previously,<sup>12,13</sup> the energy cut-off of the  $H_2$  formation is around 100 kcal/mol, while the peak of the distribution is only about 15 kcal/mol, indicating that most available energy of this channel is deposited into the product internal degrees of freedom. There are at least three possible dissociation pathways for the  $H_2$  formation channel: the  $H_2$  +  $c\text{-}C_3H_4$  channel, the  $H_2$  + propyne channel and the  $H_2$  + allene channel. The  $H_2$  +  $c\text{-}C_3H_4$  process is believed to be the most favorable because this pathway is more straightforward dynamically than the other two pathways.

TOF spectra at mass 14 and mass 28 have been observed in this work using the VUV ionization detection scheme. These TOF signals can be assigned to the  $C_2H_4$  +  $CH_2$  channel. A single kinetic energy distribution is used to fit the TOF spectra at both mass 28 and mass 14, indicating that the

TOF signals observed at mass 28 and mass 14 are truly momentum matched and clearly from the  $C_2H_4 + CH_2$  channel. The dynamical source of this dissociation channel is quite interesting. There are two possible dissociation mechanisms for this channel: a simultaneous breakup of the two C–C bonds and the ring-opening followed by a C–C bond cleavage. It is not immediately clear which of the above two mechanisms is more plausible based on the present experimental data. Further theoretical studies are required in order to clarify the mechanism of this dissociation channel.

TOF spectra at mass 15 and mass 27 have also been observed. Since small dissociative ionization is expected at the photon energy used in the detection, these detected signals at mass 15 and mass 27 can be assigned to the  $CH_3 + C_2H_3$  from the cyclopropane. From simulating the TOF data at both mass 15 and mass 27, it is clear that these two products are momentum matched. The average kinetic energy release is quite low, indicating that the available energy of this process is mostly deposited into the product internal degrees of freedom. Dynamically, the observation of this channel is also quite interesting since this dissociation channel requires an H atom migration prior to dissociation. An interesting dynamical issue in this dissociation channel is whether the C–C ring opens first followed by an H migration, or H atom migration occurs first, which also needs further theoretical investigations.

It is expected that soft VUV ionization will also cause much less fragmentation than electron impact ionization, thus making the detection and analysis of multiple channel reaction processes more straightforward. Since the VUV synchrotron radiation is tunable, different photon energies are conveniently used to ionize the reaction products in order to clarify the dissociative ionization problem. Figure 24 shows the TOF spectra detected at masses 26, 27 and 28 from cyclopropane photodissociation at 157 nm with three different VUV ionization energies from 11 eV to 13 eV. From this figure, it is quite obvious that the dissociative ionization is significantly reduced as the VUV photon ionization energy decreases. The signals at mass 26 in the TOF spectra are clearly due to dissociative ionization from the parent products at mass 28 ( $C_2H_4$ ) and mass 27 ( $C_2H_3$ ). Signals at mass 26 are relatively significantly smaller at 11 eV, in comparison with that at 12 eV or 13 eV ionization. Furthermore, it is interesting to see that the ion signal at mass 26 is relatively larger than that at mass 27. This is likely due to the fact that the  $C_2H_4^+$  ion is more likely to crack into  $C_2H_2^+$  rather than  $C_2H_3^+$  at the ionization energies used in this work. This observation

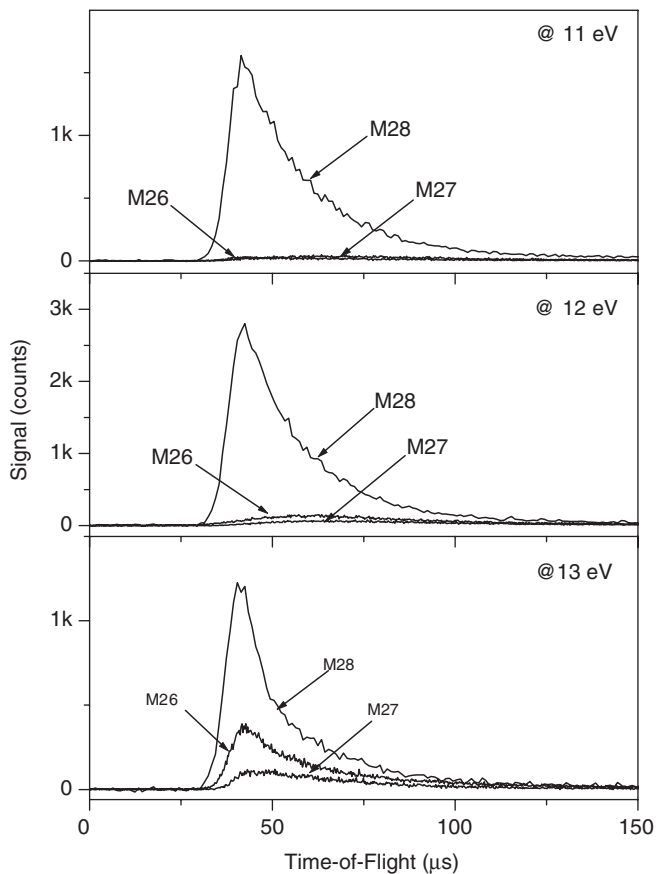


**Fig. 24.** TOF spectra of masses 26, 27 and 28 products obtained using different VUV photoionization energies.

can be explained using a breakdown diagram of the different dissociation patterns at different ionization energies  $C_2H_4^+$ .<sup>84–86</sup>

From a rough estimation, the  $C_2H_4 + CH_2$  channel is found to be the dominant channel with 68% contribution, while the  $CH_3 + C_2H_3$  channel and the H formation channel are both found to be significant with 17% and 14% contributions respectively. The  $H_2$  formation is, however, minor with only about 1% contribution.

From the above study, the advantage using VUV ionization is quite obvious, especially the much smaller dissociative ionization makes minor channels, such as  $CH_3 + C_2H_3$ , clearly detectable while these signals would be smeared in the electron impact ionization detector by dissociative ionization

signals. In addition, we have also compared the detection sensitivity of this apparatus based on the VUV ionization with that of the universal molecular beam apparatus based on the electron impact ionization by using this system under similar experimental conditions. The newly built VUV apparatus is at least as sensitive as the improved universal apparatus described above if not more sensitive. This provides us the confidence that this apparatus will be very useful in the future for unique crossed molecular beam studies.

### 3.2.2. $\text{CH}_3\text{Cl}$ at 157 nm

Three different channels have been observed for this system.<sup>87</sup> These signals observed at mass 15 and 35 can be easily assigned to the  $\text{CH}_3 + \text{Cl}$  channel. The product translational energy for this channel is shown in Fig. 25. The dynamics of this dissociation channel is very much similar to the photodissociation of  $\text{CH}_3\text{Cl}$  through A band excitation (at 193.3 nm and longer wavelengths). The repulsive potential energy surfaces with  $\sigma^*$  character are responsible for the dissociation dynamics of A band excitation, which results in high translational energy deposition. Since the absorption spectra of the B band shows some diffuse vibration structures, the excited electronic state is clearly a fast predissociative state (ten femtoseconds or so). Therefore, the dissociation of  $\text{CH}_3\text{Cl}$  at 157.6 nm wavelength occurs via fast predissociation through a pure repulsive surface, which is likely via the  $\sigma^*$  repulsive state. The dynamics of this dissociation channel are also similar to the photodissociation of  $\text{CH}_3\text{I}$  through the A band and B band transition, in which a large fraction of the available energy is also deposited into the translational degree of freedom.<sup>88</sup>

The H atom formation channel ( $\text{H} + \text{CH}_2\text{Cl}$ ) is also observed. TOF spectra were measured at mass 49 and mass 1, which can be simulated using the  $P(E_T)$  shown in Fig. 25. This  $P(E_T)$  peaks at 62 kcal/mol (77% of the available energy), also indicating a fast predissociation mechanism via a repulsive surface for the H atom elimination. This mechanism is similar to the Cl atom elimination process. In the previous investigations of the H atom product by Tonokura *et al.*,<sup>89</sup> the H atom generated from photodissociation of  $\text{CH}_3\text{Cl}$  at 157.6 nm has two components: a fast component and a slow component. The relative branching ratio of this  $\text{H} + \text{CH}_2\text{Cl}$  channel is at least 10 times smaller than the  $\text{CH}_3 + \text{Cl}$  channel.

In addition to the two atomic elimination channels, another interesting molecular elimination channel has also been clearly observed. TOF spectra of mass 14 at the laboratory angle of  $70^\circ$  with ionization photon energy from

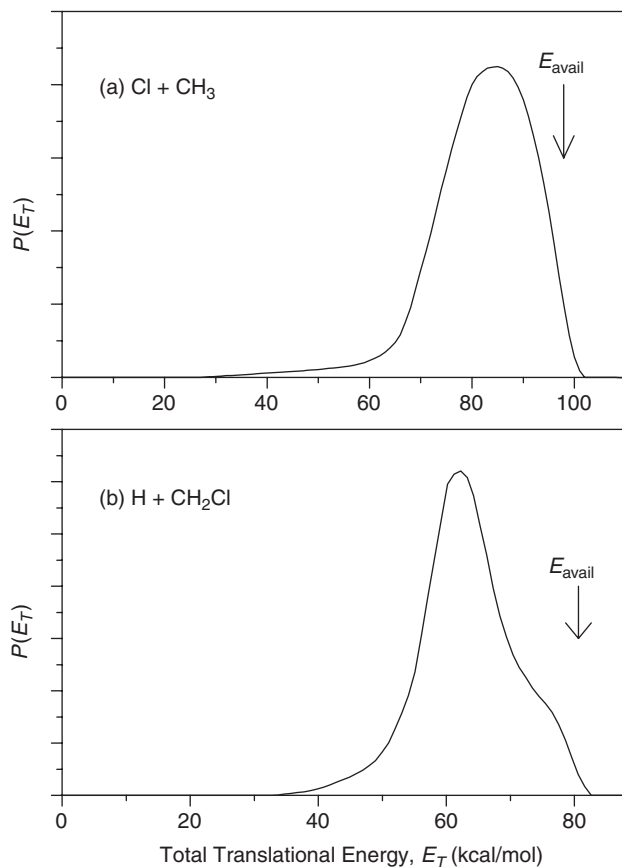


**Fig. 25.** (a) The translational energy distribution for the  $\text{CH}_3 + \text{Cl}$  channel. (b) The translational energy distribution for the  $\text{H} + \text{CH}_2\text{Cl}$  channel.

10.3 eV to 13.8 eV have been measured. Mass 14 signal from the dissociative ionization of  $\text{CH}_3$  product should not be significant at ionizing photon energy  $\leq 14$  eV since the adiabatic threshold of  $\text{CH}_3 + h\nu \rightarrow \text{CH}_2^+ + \text{H} + \text{e}^-$  is 15.12 eV.<sup>90</sup> Because the U9 undulator photon beam contains small amount of high energy photons which could lead to dissociative ionization of the  $\text{CH}_3$  radical, the extent of dissociative ionization of  $\text{CH}_3$  by the undulator beam photons was checked carefully by measuring the mass 14 and mass 15 signals for the  $\text{CH}_3$  radical from the photodissociation of dimethyl ether ( $\text{CH}_3\text{-O-CH}_3$ ) at 157.6 nm. The signal at mass 14 is less than 0.3% of the signal at mass 15 under similar conditions to the  $\text{CH}_3\text{Cl}$  experiment,

indicating dissociative ionization of  $\text{CH}_3$  caused by VUV ionization is very small. This result implies that the signal observed at mass 14 ( $\text{CH}_2^+$ ) from photodissociation of  $\text{CH}_3\text{Cl}$  is due to primary  $\text{CH}_2$  product, not dissociation ionization of the  $\text{CH}_3$  radical. Clearly, the shapes of the TOF spectra at mass 14 are significantly different from those at mass 15. Two peaks (fast/slow) are observed at higher ionizing photon energies. The fast peak becomes weaker and almost disappears at lower ionizing photon energy. The translational energy distributions used in simulating the two peaks are shown in the upper panel in Fig. 26. Similar double peak structures are also observed in the TOF spectra at mass 36 ( $\text{HCl}^+$ ) by both photoionization and electron impact ionization. Two  $P(E_T)$ 's are used to simulate the mass 14 TOF spectra at ionizing photon energy from 10.3 to 13.8 eV. The relative

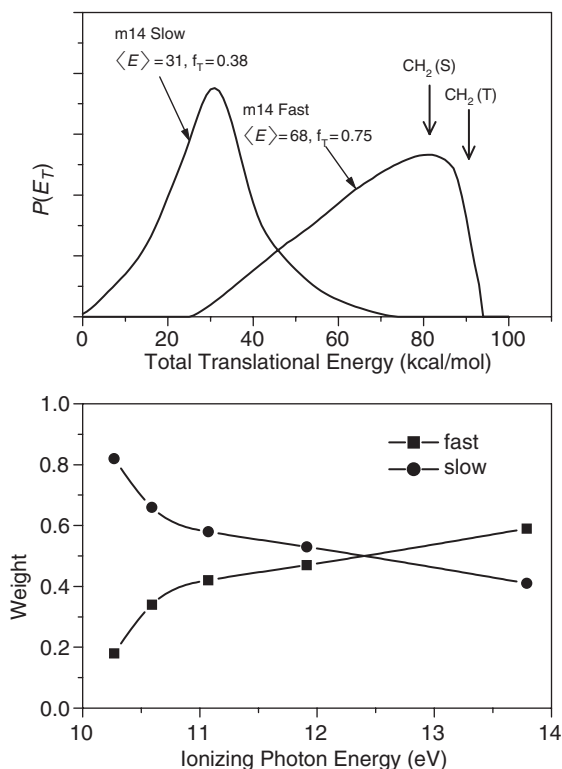


**Fig. 26.** (a) The translational energy distributions for fast and low  $\text{CH}_2 + \text{HCl}$  channels. (b) The weighting of the fast and slow  $\text{CH}_2 + \text{HCl}$  channels used in the simulation at various ionizing photon energy.

branching of fast/slow  $\text{CH}_2 + \text{HCl}$  channels are shown in the lower panel in Fig. 26. The TOF spectra at mass 36 detected at photon energy from 15 eV to 21 eV can also be simulated using the same  $P(E_T)$ 's. The momentum match for the mass 14 and mass 36 products strongly suggests that signals at mass 14 and mass 36 should come from the  $\text{CH}_2 + \text{HCl}$  channel. The fast channel is assigned to the  $\text{CH}_2(\tilde{X}^3B_1) + \text{HCl}$  channel, the slower channel is assigned to the  $\text{CH}_2(\tilde{a}^1A_1) + \text{HCl}$  channel.

Similar to the other two atomic channels, the majority (75%) of the available energy is deposited to the translational degree of freedom for the  $\text{CH}_2(\tilde{X}^3B_1) + \text{HCl}$  channel, implying that this channel is more or less a direct and fast dissociation process. This is quite surprising for a molecular elimination channel since molecular elimination processes normally exhibit more statistical type behavior in which majority of the available energy is deposited into the internal degrees of freedom. For the slow  $\text{CH}_2(\tilde{a}^1A_1) + \text{HCl}$  channel, the  $P(E_T)$  peaks at about 30 kcal/mol with an available energy of about 80 kcal/mol. Therefore, the majority (~63%) of the available energy is distributed into the internal degrees of freedom for this channel, which implies that the dissociation of this channel is likely more statistical, unlike other dissociation pathways.

#### 4. Future Outlook

We have witnessed significant progresses in the studies of crossed molecular reaction dynamics during the last decade or so. The improvement of the universal crossed beam apparatus based on electron impact ionization in our laboratory has propelled us into the studies of multiple channel dynamics of complex chemical reactions. Further improvement on this technique is certainly possible, but there are limits for such improvement since the basic limitation of detection sensitivity for this technique is from the electron space charge problem in the electron impact ionizer, in which electrons can only be packed to a limited density because electrons repel each other. However, some improvements are still possible, such as, closer detection distance and even larger quadrupole rod assembly. There is a possibility to improve the detection sensitivity by a few times, but that will have to sacrifice either the energy resolution or quadrupole mass range in the apparatus. Such improvement is certainly desirable if one wants to study radical-radical reactions.

The development of molecular beam apparatus based on VUV ionization has been a significant step in the studies of molecular reaction dynamics.